nature chemistry

ARTICLES

PUBLISHED ONLINE: 9 JANUARY 2011 | DOI: 10.1038/NCHEM.948

Carbon oxidation state as a metric for describing the chemistry of atmospheric organic aerosol

Jesse H. Kroll[1,2]*, Neil M. Donahue[3], Jose L. Jimenez[4], Sean H. Kessler[2], Manjula R. Canagaratna[5], Kevin R. Wilson[6], Katye E. Altieri[7], Lynn R. Mazzoleni[8], Andrew S. Wozniak[9], Hendrik Bluhm[6], Erin R. Mysak[6†], Jared D. Smith[6†], Charles E. Kolb[5] and Douglas R. Worsnop[5,10,11,12]

A detailed understanding of the sources, transformations and fates of organic species in the environment is crucial because of the central roles that they play in human health, biogeochemical cycles and the Earth's climate. However, such an understanding is hindered by the immense chemical complexity of environmental mixtures of organics; for example, atmospheric organic aerosol consists of at least thousands of individual compounds, all of which likely evolve chemically over their atmospheric lifetimes. Here, we demonstrate the utility of describing organic aerosol (and other complex organic mixtures) in terms of average carbon oxidation state, a quantity that always increases with oxidation, and is readily measured using state-of-the-art analytical techniques. Field and laboratory measurements of the average carbon oxidation state, using several such techniques, constrain the chemical properties of the organics and demonstrate that the formation and evolution of organic aerosol involves simultaneous changes to both carbon oxidation state and carbon number.

The oxidation of organic species in the atmosphere is central to several key environmental chemical processes that directly influence human health and global climate. These include the degradation of pollutants, the production of toxic species such as ozone, and the formation and evolution of fine particulate matter (aerosols). This last topic is inextricably linked to the oxidation of atmospheric organics, because organic aerosol material makes up a substantial fraction (20–90%) of submicrometre aerosol mass[1]. A large fraction of organic particulate matter comprises secondary organic aerosol, formed from the oxidation of gas-phase organic species[2,3].

Current state-of-the art models have difficulty in predicting the loadings, spatial and temporal variability, and degree of oxidation of ambient organic aerosol, indicating a gap in our understanding of atmospheric oxidation processes. The oxidation mechanisms for light volatile organic compounds are relatively straightforward, with the canonical example being conversion of methane into formaldehyde, CO and ultimately CO_2 (ref. 4). However, the oxidation of larger organics associated with secondary organic aerosol involves a much larger number of reaction pathways, intermediates and products, the detailed characterization of which is beyond the capabilities of most analytical techniques. This extreme chemical complexity has prevented the precise measurement and prediction of the oxidation dynamics associated with the formation and evolution of atmospheric organic aerosol.

In this Article, we describe a new metric for the degree of oxidation of atmospheric organic species, the average carbon oxidation state ($\overline{OS}_C$), a quantity that necessarily increases upon oxidation and is measurable using several modern analytical techniques. The general concept of average carbon oxidation state has been used previously in other contexts, such as in soil chemistry for the measurement of ecosystem oxidative ratios[5], in botany for the estimation of growth yields[6], in wastewater treatment for the determination of degradation mechanisms[7] and in atmospheric chemistry to describe individual oxidation products of methane[8] and α-pinene[9]. To our knowledge $\overline{OS}_C$ has not been used to describe the evolving composition of a complex mixture of organics undergoing dynamic oxidation processes.

Here we show that $\overline{OS}_C$, when coupled with carbon number (n_C), provides a framework for describing the chemistry of organic species in the atmosphere, and in particular atmospheric organic aerosol. These two fundamental quantities can be used to constrain the composition of organic aerosol and, moreover, to uniquely define key classes of atmospheric reactions, providing insight into the oxidative evolution of atmospheric organics.

Results

Definition of $\overline{OS}_C$ and relationship with n_C. The oxidation state of carbon is defined as the charge a carbon atom would take if it were to lose all electrons in bonds with more electronegative atoms, but gain all electrons in bonds with less electronegative atoms. This quantity will necessarily increase in oxidizing environments such as the Earth's atmosphere. The oxidation states of individual carbon atoms within a molecule, or within a mixture of molecules, may change differently upon oxidation, but the average

[1]Department of Civil and Environmental Engineering, Massachusetts Institute of Technology, Cambridge, Massachusetts 02139, USA, [2]Department of Chemical Engineering, Massachusetts Institute of Technology, Cambridge, Massachusetts 02139, USA, [3]Center for Atmospheric Particle Studies, Carnegie Mellon University, Pittsburgh, Pennsylvania 15213, USA, [4]Cooperative Institute for Research in the Environmental Sciences and Department of Chemistry and Biochemistry, University of Colorado, Boulder, Colorado 80309, USA, [5]Center for Aerosol and Cloud Chemistry, Aerodyne Research, Billerica, Massachusetts 01821, USA, [6]Chemical Sciences Division, Lawrence Berkeley National Laboratory, Berkeley, California 94720, USA, [7]Department of Geosciences, Princeton University, Princeton, New Jersey 08544, USA, [8]Department of Chemistry, Michigan Technological University, Houghton 49931, Michigan, USA, [9]Department of Chemistry and Biochemistry, Old Dominion University, Norfolk, Virginia 23529, USA, [10]Department of Physics, University of Helsinki, Helsinki, Finland, [11]Finnish Meteorological Institute, Helsinki, Finland, [12]Department of Physics, University of Eastern Finland, Kuopio, Finland; †Present address: L.J. Smith and Associates, 9515 Brooks Drive, Rogers, Arkansas 72756, USA (J.D.S.); Straus Center for Conservation and Technical Studies, Harvard Art Museums, Cambridge, Massachusetts 02138, USA (E.R.M.). *e-mail: jhkroll@mit.edu

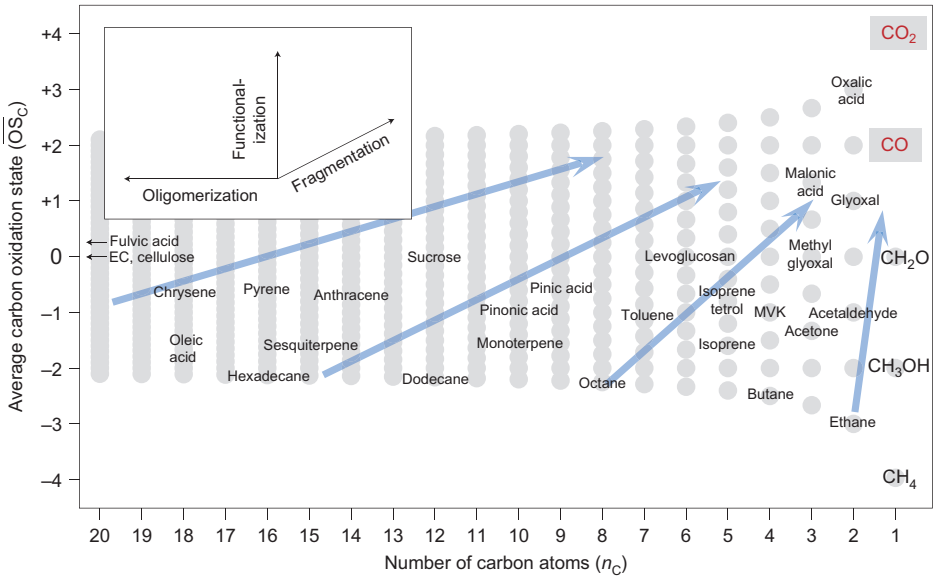

Figure 1 | Possible combinations of average carbon oxidation state ($\overline{OS}_C$) and number of carbon atoms (n_C) for stable organic molecules. Any organic species can be placed in this two-dimensional space; the locations of key atmospheric organics (and common surrogate species) are shown. The vast majority of known atmospheric species are reduced ($\overline{OS}_C \leq 0$), with only the smallest compounds having higher oxidation states. Inset: vectors corresponding to key classes of reactions of atmospheric organics: functionalization (addition of polar functional groups), fragmentation (cleavage of C–C bonds) and oligomerization (covalent association of two organic species). The combination of these reaction types leads to complex movement through $\overline{OS}_C$–n_C space; however, the inevitable increase in $\overline{OS}_C$ with atmospheric oxidation implies that, given enough time, organics will generally move up and to the right (blue arrows), towards CO_2.

oxidation state of the carbon ($\overline{OS}_C$) must increase. Thus the quantity $\overline{OS}_C$ is an ideal metric for the degree of oxidation of organic species in the atmosphere, and serves as a key quantity to describe organic mixtures that are as chemically complex as organic aerosol.

In the atmosphere, the increase in carbon oxidation state arises from the formation of bonds between carbon and oxygen (and other electronegative elements) and/or the breaking of bonds between carbon and hydrogen (and other electropositive elements). This influence of both electronegative and electropositive atoms has important implications for atmospheric oxidation. First, metrics of oxidation that involve only one of these, such as the oxygen-to-carbon molar ratio (O/C), may not accurately capture the degree of oxidation of the organics. For example, the oxidation of an alcohol to a carbonyl involves no change in O/C; conversely, O/C may be affected dramatically by non-oxidative processes such as hydration or dehydration. Second, because the oxidation state of a carbon atom is not affected by bonds to other carbon atoms, the number of carbons in a molecule (n_C) governs the range of possible values of $\overline{OS}_C$.

Figure 1 shows the possible combinations of $\overline{OS}_C$ and n_C for stable organic molecules with a contiguous carbon skeleton, as governed by chemical valence rules. Also shown are the locations in this two-dimensional space of organics that are either important in the atmosphere or are commonly used as surrogates for atmospheric species. The vast majority of these species are reduced ($\overline{OS}_C \leq 0$); most known compounds with higher average oxidation states are small, with only 1–3 carbon atoms.

Reactions that govern the chemical transformation of atmospheric organics and the evolution of organic aerosol involve movement in $\overline{OS}_C$–n_C space. The oxidative transformation of atmospheric organics can occur within a range of chemical environments, including in the gas phase, at the gas–particle interface or within the bulk organic or aqueous phase; non-oxidative transformations (such as accretion reactions) may also occur. These chemistries can all be described in terms of three key classes of reactions (Fig. 1, inset): functionalization (the oxidative addition of polar functional groups to the carbon skeleton), fragmentation (the oxidative cleavage of C–C bonds) and oligomerization (the association of two organic molecules). These reactions are defined uniquely by the changes to $\overline{OS}_C$ and n_C of the organics, so the $\overline{OS}_C$–n_C space is an ideal conceptual framework to describe the chemical changes that atmospheric organics undergo upon oxidation. This fundamental chemical nature of the $\overline{OS}_C$–n_C space distinguishes it from other emerging two-dimensional treatments of organic aerosol[10–12]. Such frameworks are extremely useful for describing or modelling aerosol based on experimental measurements, but they are based upon quantities that cannot be related to these general classes of chemical reactions in a straightforward manner, and so they provide limited insight into the nature of atmospheric chemical transformations (see Supplementary Information for a more detailed discussion).

In $\overline{OS}_C$–n_C space, atmospheric oxidation has an inherent directionality. Because the carbon oxidation state must increase upon oxidation, the ultimate end product of the oxidation of organic species (given enough time) is necessarily CO_2 ($OS_C = +4$). Reaching this oxidative end product requires both the addition of oxygen-containing moieties (increasing $\overline{OS}_C$), and the breaking of C–C bonds (decreasing n_C). The oxidation of atmospheric organic species therefore involves an overall movement towards the upper right of Fig. 1 (blue arrows). Leftwards movement towards larger carbon numbers (oligomer formation) certainly occurs in many cases[3], but even the high-molecular-weight products of accretion reactions are susceptible to oxidative degradation[13] and ultimately will form CO_2.

Measurements of $\overline{OS}_C$. A critical strength of $\overline{OS}_C$ as a metric of atmospheric processing of organics, in addition to the fact that it must increase upon oxidation, is that it can be measured routinely using state-of-the-art analytical techniques. Carbon oxidation state is determined by the identity and abundance of non-carbon

atoms in the organic compound(s):

$$\overline{OS}_C = -\sum_i OS_i \frac{n_i}{n_C} \quad (1)$$

in which the summation is over all non-carbon elements, OS_i is the oxidation state associated with element i, and n_i/n_C is the molar ratio of element i to carbon. Thus the measurement of $\overline{OS}_C$ requires that all non-carbon elements in the sample be characterized in terms of their relative abundances and oxidation states.

Atmospheric organics are primarily composed of carbon, hydrogen (OS = +1) and reduced oxygen (OS = –2), so equation (1) can often be simplified to

$$\overline{OS}_C \approx 2\,O/C - H/C \quad (2)$$

This relation is exact for organics made up of only carbon, hydrogen and most oxygen-containing functional groups (alcohols, carbonyls, carboxylic acids, ethers and esters). The presence of peroxide groups (in which the oxygen atoms have an oxidation state of –1) and heteroatoms (which can have a range of oxidation states) introduces deviations from this relation. These can be corrected by measuring individual functional groups; however, such moieties generally represent a minor component of organic aerosol (on a per-carbon basis), so such errors tend to be small. For example, the independent determination of O/C and peroxide content[14] allows for an accurate determination of $\overline{OS}_C$ in secondary organic aerosol formed from isoprene ozonolysis; however, even for such a peroxide-rich system, equation (2) yields an $\overline{OS}_C$ that is within 0.1 of the exact value from equation (1). Similarly, the measurement of nitrogen-containing functional groups allows for nitrogen atoms to be explicitly included in the determination of $\overline{OS}_C$, although organic nitrogen is a sufficiently small fraction of organic particulate matter that this has a relatively minor effect on calculated $\overline{OS}_C$ (see Supplementary Information). Nonetheless, in some cases these moieties might be present in relatively high abundances, so their effect on measured $\overline{OS}_C$ is an important topic for future research.

Here, we focus on the simplified determination of $\overline{OS}_C$ from equation (2), based on measurements of O/C and H/C only. A number of analytical techniques can be used to determine elemental ratios, and therefore $\overline{OS}_C$, of atmospheric particulate matter. These include combustion analysis (CHNS)[15–17], ultrahigh-resolution mass spectrometry with electrospray ionization (ESI)[14,18–21], nuclear magnetic resonance (NMR) spectroscopy[22], Fourier transform infrared spectroscopy (FTIR)[23], X-ray photoelectron spectroscopy (XPS; E. R. Mysak *et al.*, manuscript in preparation) and high-resolution electron impact aerosol mass spectrometry (HR–AMS)[24–29]. Each technique has its own strengths and weaknesses for characterizing organic aerosol. For example, CHNS analysis is accurate and universal, but requires large amounts of collected organics, and oxygen content is usually determined only by subtraction. ESI can provide exact elemental ratios of individual compounds within a complex mixture, and requires very little sample volume; however, it is a selective ionization technique, with response factors that may vary widely among different species. HR–AMS is a sensitive, online technique for measuring elemental ratios in real time, but is not as accurate as other techniques, because it requires uncertain empirical corrections to account for biases during ion fragmentation[24]. Because of the uncertainties associated with each technique, it is useful to examine results from a range of elemental analysis approaches to obtain an accurate, complete picture of the carbon oxidation state of organic aerosol.

Atmospheric organic aerosol and $\overline{OS}_C$. Table 1 presents compiled measurements of the mean carbon oxidation state of organic aerosol, taken from measurements of O/C and H/C using the three most widely used elemental analysis techniques (CHNS, ESI and HR–AMS). These include measurements of ambient organic aerosol, ambient aerosol fractions (by physical extraction or factor analysis) and laboratory-generated primary or secondary organic aerosol. A consistent picture emerges from these results, with the $\overline{OS}_C$ of organic aerosol ranging from –2 to +1, depending on the level of atmospheric aging. Individual species in organic aerosol, such as oxalate and other highly oxidized species, may have oxidation states greater than +1, but all available data suggest that the average carbon oxidation state of organic aerosol rarely exceeds this value. Even classes of organics that are generally considered to be highly oxidized, such as humic-like substances (HULIS) and oxygenated organic aerosol (OOA), have an $\overline{OS}_C$ below +1. It appears that more highly oxidized carbon is found predominantly in the gas phase, presumably because species with several (>3) adjacent carbonyl groups are thermodynamically or photochemically unstable, and will rapidly decompose to smaller species.

Table 1 | Measurements of $\overline{OS}_C$ of organic aerosol.

	$\overline{OS}_C$	Technique	Ref.
Ambient organic aerosol			
Urban/anthropogenic (Mexico City)	−1.6 to +0.1	AMS	24
Remote/biogenic (Amazonian rainforest)	−0.9 to −0.2	AMS	29
Aged (Whistler Mountain)	−0.6 to +0.6	AMS	28
Ambient aerosol fractions			
Hydrocarbon-like organic aerosol (HOA)	−1.7 to −1.6	AMS	24
Semivolatile oxygenated organic aerosol (SV-OOA)	−0.5 to 0.0	AMS	24
Low-volatility oxygenated organic aerosol (LV-OOA)	+0.5 to +0.9	AMS	24
Humic-like substances (HULIS)	−0.4 to −0.3	CHNS	16, 17
Water-soluble organic carbon (WSOC) in rainwater	−0.9 to −0.7	ESI	18
WSOC in aerosol	−1.0	ESI	20
WSOC in fogwater	−0.7	ESI	21
Primary organic aerosol			
Vehicle exhaust (gasoline, diesel)	−2.0 to −1.9	AMS	24
Biomass burning aerosol	−1.0 to −0.7	AMS	24
Secondary organic aerosol			
Monoterpene + O_3	−1.1 to −0.5	AMS, ESI	19, 24, 25, 27
Isoprene + OH or O_3	−0.8 to −0.2	AMS, ESI	14, 24, 27
Monoaromatics + OH	−0.9 to +0.1	AMS	24, 27
Alkane/alkene photo-oxidation	−0.7 to −0.4	AMS, CHNS	15, 26

Values listed are the $\overline{OS}_C$ ensemble averages for a given sample; $\overline{OS}_C$ values of individual molecules within a sample may be distributed around these averages, as illustrated in Fig. 2. Techniques listed are high-resolution aerosol mass spectrometry (AMS), ultrahigh resolution mass spectrometry with electrospray ionization (ESI) and combustion analysis (CHNS).

Figure 2 shows the approximate area of $\overline{OS}_C$–n_C space corresponding to atmospheric organic aerosol, based upon the $\overline{OS}_C$ measurements shown in Table 1, and determinations of n_C from ultrahigh-resolution ESI or known relationships between volatility and carbon number[30]. Results from AMS/volatility measurements and from ESI data are remarkably consistent, placing aerosol components in the areas of $\overline{OS}_C$–n_C space corresponding to large and/or polar organics. Oxidized particle-phase organics (HULIS and OOA) lie between the large, reduced species ($n_C \geq 5$, $\overline{OS}_C < -1$) and the oxidative endpoint CO_2. Thus, secondary organic aerosol is not the product of only a few select hydrocarbons, but is rather formed in the oxidation of most organic species. The only reduced organic species unlikely to contribute to aerosol formation

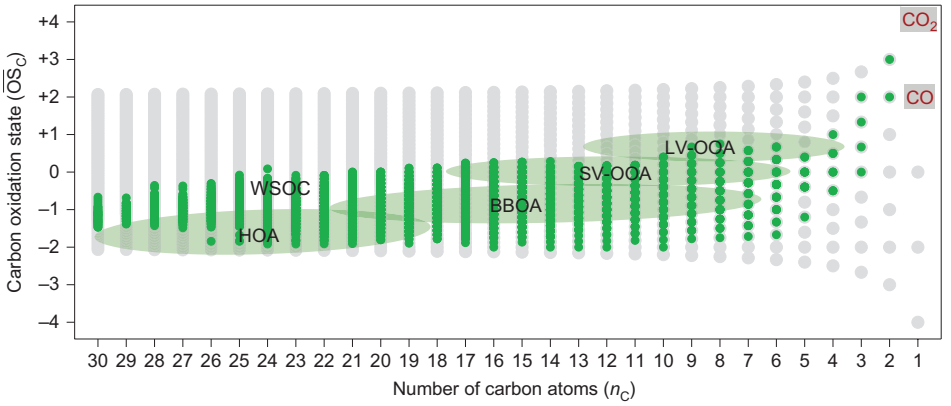

Figure 2 | Location in $\overline{OS}_C$–n_C space of organic aerosol, based upon $\overline{OS}_C$ measurements of organic aerosol. Green circles: locations of individual components of water-soluble organic compounds (WSOC), as measured by ultrahigh-resolution mass spectrometry with ESI[20,21]. Green shaded ovals: locations of different organic aerosol classes, as determined from factor analysis of AMS data[24] and estimation of n_C from volatility measurements[30]. Hydrocarbon-like organic aerosol (HOA) and biomass burning organic aerosol (BBOA) correspond to primary particulate matter directly emitted into the atmosphere. Semivolatile and low-volatility oxidized organic aerosol (SV-OOA and LV-OOA) correspond to 'fresh' and 'aged' secondary aerosol produced by multistep oxidation reactions[11]. These aerosol species and types fall along the rough oxidation trajectories shown in Fig. 1, according to their degree of oxidation. The apparent absence of large ($n_C \geq 5$), highly oxidized ($\overline{OS}_C > 1$) organics in organic aerosol is probably due to the thermodynamic and photochemical instability of such species.

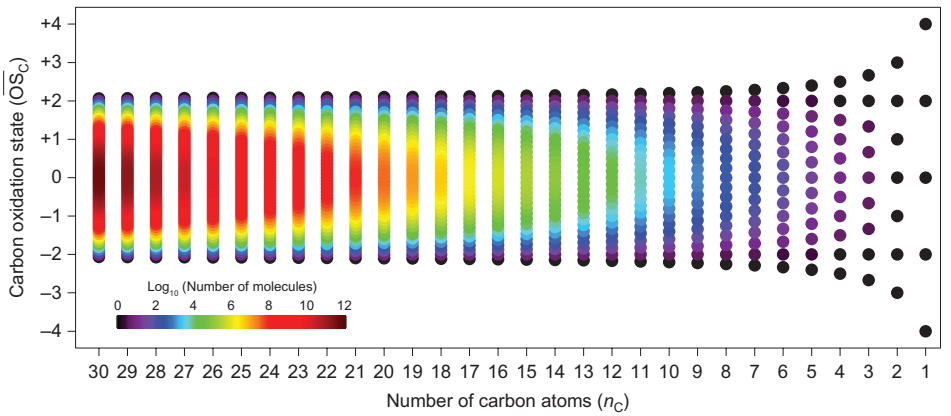

Figure 3 | Chemical complexity of organics as a function of oxidation state and carbon number. Points are coloured by the logarithm (base 10) of the number of possible compounds at a given $\overline{OS}_C$ and n_C, assuming an unbranched, acyclic carbon skeleton, and the addition of carbonyl, alcohol and acid groups only. Including a wider range of carbon skeletons or functional groups will lead to a dramatically steeper increase in chemical complexity with $\overline{OS}_C$ and n_C (ref. 31).

upon oxidation are small (four carbons or fewer), though even those might form organic aerosol through oligomerization reactions. The potential formation of aerosol from such a wide variety of organic species is a likely contributor to underestimates of secondary organic aerosol concentrations, because models (and the experiments on which they are based) typically focus on only a few select aerosol precursors[3].

Chemical complexity. Most points in $\overline{OS}_C$–n_C space represent a multitude of compounds; for example, the point corresponding to $n_C = 2$ and $\overline{OS}_C = -1$ includes acetylene (C_2H_2), acetaldehyde (CH_3CHO) and ethylene glycol ($HOCH_2CH_2OH$) (these compounds are related to each other by the nominal gain/loss of H_2O, which involves no change in $\overline{OS}_C$ or n_C). The number of possible chemical structures (chemical complexity) is a strong function of not only n_C (ref. 31) but also oxidation state. Figure 3 shows the number of possible structures for just a single carbon skeleton (an unbranched, acyclic carbon chain), with carbonyl, alcohol and/or carboxylic acid groups. For a given carbon number, only one structure (the *n*-alkane) is possible at the lowest $\overline{OS}_C$ value. The number of possible structures then increases rapidly with $\overline{OS}_C$, due to the combinatorial addition of different functional groups to different carbon atoms. The maximum in chemical complexity is located at $\overline{OS}_C = 0$; for molecules in which the average carbon atom is oxidized ($\overline{OS}_C > 0$), the number of possible chemical structures then decreases with increasing oxidation state.

Many of the compounds that make up organic aerosol (Fig. 2) lie in the region of maximum chemical complexity (Fig. 3). This underscores the enormous experimental and theoretical challenges associated with describing aerosol in terms of its individual molecular components. The number of oxidized organics ($-1 \leq \overline{OS}_C \leq +1$) is far greater than can reasonably be constrained by measurements of ambient species, laboratory studies of reaction rates and products, or explicit models of the fate of individual atmospheric compounds. The sheer number of possible species in organic aerosol indicates that a completely speciated approach is probably not feasible for a generalized description of organic aerosol. This is particularly true for regional or global air-quality and climate models, which instead require concise descriptions of atmospheric organic mixtures in terms of measurable ensemble quantities such as $\overline{OS}_C$.

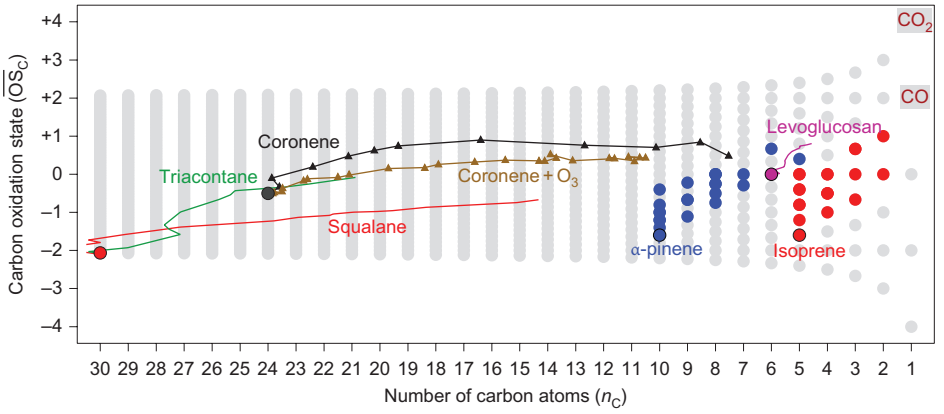

Figure 4 | Oxidation trajectories in $\overline{OS}_C$–n_C space, as determined from laboratory studies of oxidation reactions. OH is used as the oxidant except where noted. Results from three independent experimental and analytical approaches are shown: the heterogeneous oxidation of pure organic particles, measured with HR-AMS (solid lines)[38,39]; the heterogeneous oxidation of thin films, measured by XPS (marked by filled triangles; E. R. Mysak *et al.*, manuscript in preparation) and the gas-phase oxidation of hydrocarbons, measured by various techniques to speciate gas- and particle-phase organics (filled circles)[42–48]. In most cases, oxidation initially adds functional groups to the carbon skeleton (upwards movement), but later oxidation steps involve a decrease in n_C through the breaking of C–C bonds (movement upwards and to the right), indicating the crucial role of fragmentation reactions in photochemical aging and aerosol evolution. For clarity, only monomeric products are shown; the formation of oligomers also entails initial movement to the left, but as these oligomeric species are composed of monomeric subunits, they will display the same general trajectories upon oxidation.

Oxidative transformations of atmospheric organics. To be accurate, such concise descriptions must properly capture the oxidation mechanisms of atmospheric organic species. This underscores the critical importance of the measurement of selected individual species within organic aerosol to characterize reaction pathways, as well as to identify aerosol sources and toxic species. Insight into oxidation mechanisms can be obtained from experimental studies of the multigenerational oxidation products of individual organics. Results from several such studies, mapped onto $\overline{OS}_C$–n_C space, are shown in Fig. 4. These results were obtained using a range of analytical techniques, including ensemble measurements of condensed-phase organics (HR–AMS and XPS) and speciated measurements of gas- and particle-phase organics (various mass spectrometric techniques).

For all systems studied (Fig. 4), oxidation leads to increased functionality on the carbon skeleton (higher $\overline{OS}_C$) and, after only a few (1–4) generations of oxidation, a decrease in carbon number of the original carbon skeleton (lower n_C). Fragmentation reactions are therefore key processes in the oxidative aging of atmospheric organics. This is particularly true for oxidized species, which have oxygen-containing (electron-withdrawing) groups that weaken adjacent C–C bonds[32]. This increase in $\overline{OS}_C$ towards CO_2 can occur via multiple reaction pathways, as illustrated by the numerous individual products of isoprene and α-pinene oxidation (circles in Fig. 4). The ensemble measurements (lines in Fig. 4) constrain the mean values of $\overline{OS}_C$, with individual compounds spanning a range in oxidation state, carbon number and volatility.

Discussion

The oxidation of organics has long been viewed as a source of atmospheric organic aerosol through secondary organic aerosol formation. However, the ultimate dominance of fragmentation reactions (movement to the top right of $\overline{OS}_C$–n_C space) means that oxidation may also serve as an organic aerosol sink, because oxidized organics may fragment and volatilize upon further oxidation. The effects of such oxidative degradation reactions on atmospheric aerosol are governed by reaction rates, given the relatively short lifetime of atmospheric particulate matter through physical deposition (~1 week). This implies that better constraints on the kinetics of key organic 'aging' reactions are needed for the accurate prediction of the loadings, properties and effects of atmospheric organic aerosol.

It is known that the heterogeneous degradation of organic particulate matter by gas-phase oxidants is generally substantially slower than of gas-phase organics[33], because most particulate organics are shielded from gas-phase radicals interacting with the particle surface. Thus organic aerosol represents a 'metastable state' in which partially oxidized organics can survive for a substantial period of time, even under highly oxidizing conditions. This view of organic aerosol as a chemically recalcitrant intermediate in the oxidation of organic species resembles the emerging view of the nature of humic materials in soils and aquatic systems[34,35]. In this sense the similarities between atmospheric particulate organics and humic materials may extend well beyond their chemical complexity and physicochemical properties[22,36], to include their role as a 'transition state' of organic matter[35]. Although detailed chemical structures and transformations are likely to be quite different (for example, biological processes do not affect atmospheric organics to the extent that they do for terrestrial or aquatic organics), the similarities suggest strong commonalties in the description and experimental studies of such highly complex environmental organic mixtures.

The description of the chemistry of organic species in terms of changes to their average carbon oxidation state (a universal, unambiguous metric for the degree of oxidation of carbon-containing species) and carbon number may thus be useful for describing not only atmospheric oxidation but also other complex reactive systems. This includes the formation and evolution of humic substances in soil or aquatic systems, the combustion of complex organic species, the formation or weathering of fossil fuels, and the chemical transformation of organics in oxygen-limited environments. Such systems can involve reactions other than the oxidative processes that govern atmospheric reactions, and therefore may exhibit trajectories in $\overline{OS}_C$–n_C space different from those shown in Fig. 4. For example, reduction moves organics downwards and to the right (towards methane, $OS_C = -4$ and $n_C = 1$), whereas radical association reactions in low-oxygen environments (such as fuel-rich flames and some planetary atmospheres[37]), involve leftwards movement, towards polycyclic aromatic hydrocarbons and eventually elemental carbon ($\overline{OS}_C = 0$ and $n_C \rightarrow \infty$). The measurement of $\overline{OS}_C$ allows for the determination of these trajectories for entire mixtures, offering the potential for simple, predictive models of these exceedingly complex chemical systems.

Methods

Determination of $\overline{OS}_C$. All $\overline{OS}_C$ values reported in Table 1 and illustrated in Figs 2 and 4 were determined using equation (2). The one exception is the $\overline{OS}_C$ of secondary organic aerosol formed from the photooxidation of alkenes[15]; the high contribution of organic nitrates (N/C = 0.1) requires the explicit inclusion of nitrogen ($OS_N = +5$). A discussion of the potential errors associated with neglecting heteroatoms in equation (2) is given in the Supplementary Information.

Ensemble (average) elemental ratios were taken mostly from previously reported measurements. For AMS[24–29,38,39] and CHNS data[15–17], O/C and H/C ratios are taken directly from reported measurements. For ultrahigh-resolution ESI data[14,18–21], O/C and H/C are determined by averaging the elemental ratios of all measured CHO species, weighted by ion intensity[19]. For XPS data (C1*s* spectra at 430 eV; E. R. Mysak *et al.*, manuscript in preparation), all carbon was categorized as C = C, CH_x, C–OH, C = O or C(O)OH based on its measured binding energy, allowing for the estimation of O/C and H/C ratios. Additional details of these measurements are provided in the Supplementary Information.

Estimation of n_C. The value of n_C in ambient organic aerosol (Fig. 2) was either determined from speciated measurements (ESI data) or estimated based on measurements of particle volatility and $\overline{OS}_C$ (AMS data). This latter approach uses the SIMPOL.1 structure–activity relationship[40] to relate saturation vapour pressure, degree of oxidation and n_C (ref. 30). Vapour pressures of organic aerosol classes are based on recent *in situ* thermodenuder measurements[41]. The effects of functional groups on vapour pressure are estimated by assuming that each oxygen atom decreases the volatility of an organic molecule by a factor of 0.06 (consistent with the addition of carboxylic acids to the carbon skeleton), with oxygen content calculated from $\overline{OS}_C$ using an empirical relationship that relates elemental ratios (O/C + H/C = 2) (ref. 12). In the multigenerational oxidation experiments (AMS and XPS traces in Fig. 4), ensemble values of n_C were determined by assuming that fractional changes in carbon number are equal to the fraction of carbon remaining in the particle phase after oxidation.

Multigenerational oxidation experiments. The oxidation trajectories in $\overline{OS}_C$–n_C space (Fig. 4) were determined from laboratory studies of the oxidation of individual organic species. Gas-phase and particle-phase (monomeric) products of the OH-initiated oxidation of isoprene and α-pinene were measured by various speciated techniques[42–48]. The heterogeneous oxidation reactions of squalane, triacontane and levoglucosan were carried out by sending nucleated particles into a flow reactor, where they were exposed to high concentrations of OH generated by ozone photolysis[38,39]. Changes to particle mass and elemental ratios upon oxidation were characterized using a scanning mobility particle sizer and HR–AMS. For the oxidation of coronene (E. R. Mysak *et al.*, manuscript in preparation) vapour-deposited thin films of coronene (thickness, 4–6 Å) were exposed to varying levels of OH or O_3, and the chemical changes measured by XPS using the Ambient Pressure Photoemission Spectrometer at beamline 11.0.2 of the Advanced Light Source (Berkeley, California). The evolving abundance and type of carbon in the film was determined using C1*s* spectra at 430 eV. Experimental details are provided in the Supplementary Information.

Received 9 September 2010; accepted 11 November 2010; published online 9 January 2011

References

1. Kanakidou, M. *et al.* Organic aerosol and global climate modelling: a review. *Atmos. Chem. Phys.* **5,** 1053–1123 (2005).
2. Zhang, Q. *et al.* Ubiquity and dominance of oxygenated species in organic aerosols in anthropogenically-influenced Northern Hemisphere midlatitudes. *Geophys. Res. Lett.* **34,** L13801 (2007).
3. Kroll, J. H. & Seinfeld, J. H. Chemistry of secondary organic aerosol: formation and evolution of low-volatility organics in the atmosphere. *Atmos. Environ.* **42,** 3593–3624 (2008).
4. Logan, J. A., Prather, M. J., Wofsy, S. C. & McElroy, M. B. Tropospheric chemistry—a global perspective. *J. Geophys. Res. Oceans Atmos.* **86,** 7210–7254 (1981).
5. Masiello, C. A., Gallagher, M. E., Randerson, J. T., Deco, R. M. & Chadwick, O. A. Evaluating two experimental approaches for measuring ecosystem carbon oxidation state and oxidative ratio. *J. Geophys. Res. Biogeosci.* **113,** G03010 (2008).
6. McDermitt, D. K. & Loomis, R. Elemental composition of biomass and its relation to energy content, growth efficiency, and growth-yield. *Ann. Bot.* **48,** 275–290 (1981).
7. Vogel, F., Harf, J., Hug, A. & von Rohr, P. R. The mean oxidation number of carbon (MOC)—a useful concept for describing oxidation processes. *Water Res.* **34,** 2689–2702 (2000).
8. Jacob, D. J. *Introduction to Atmospheric Chemistry* (Princeton Univ. Press, 1999).
9. Seinfeld, J. H., Erdakos, G. B., Asher, W. E. & Pankow, J. F. Modeling the formation of secondary organic aerosol (SOA). 2. The predicted effects of relative humidity on aerosol formation in the α-pinene-, β-pinene-, sabinene-, Δ^3-carene-, and cyclohexene-ozone systems. *Environ. Sci. Technol.* **35,** 1806–1817 (2001).
10. Pankow, J. F. & Barsanti, K. C. The carbon number-polarity grid: a means to manage the complexity of the mix of organic compounds when modeling atmospheric organic particulate matter. *Atmos. Environ.* **43,** 2829–2835 (2009).
11. Jimenez, J. L. *et al.* Evolution of organic aerosols in the atmosphere. *Science* **326,** 1525–1529 (2009).
12. Heald, C. L. *et al.* A simplified description of the evolution of organic aerosol composition in the atmosphere. *Geophys. Res. Lett.* **37,** L08803 (2010).
13. Carlton, A. G. *et al.* Atmospheric oxalic acid and SOA production from glyoxal: results of aqueous photooxidation experiments. *Atmos. Environ.* **41,** 2588–7602 (2007).
14. Nguyen, T. B. *et al.* High-resolution mass spectrometry analysis of secondary organic aerosol generated by ozonolysis of isoprene. *Atmos. Environ.* **44,** 1032–1042 (2010).
15. O'Brien, R. J., Holmes, J. R. & Bockian, A. H. Formation of photochemical aerosol from hydrocarbons—chemical reactivity and products. *Environ. Sci. Technol.* **9,** 568–576 (1975).
16. Krivacsy, Z. *et al.* Study on the chemical character of water soluble organic compounds in fine atmospheric aerosol at the Jungfraujoch. *J. Atmos. Chem.* **39,** 235–259 (2001).
17. Kiss, G., Varga, B., Galambos, I. & Ganszky, I. Characterization of water-soluble organic matter isolated from atmospheric fine aerosol. *J. Geophys Res. Atmos.* **107,** 8339 (2002).
18. Altieri, K. E., Turpin, B. J. & Seitzinger, S. P. Oligomers, organosulfates, and nitrooxy organosulfates in rainwater identified by ultra-high resolution electrospray ionization FT-ICR mass spectrometry. *Atmos. Chem. Phys.* **9,** 2533–2542 (2009).
19. Bateman, A. P., Nizkorodov, S. A., Laskin, J. & Laskin, A. Time-resolved molecular characterization of limonene/ozone aerosol using high-resolution electrospray ionization mass spectrometry. *Phys. Chem. Chem. Phys.* **11,** 7931–7942 (2009).
20. Wozniak, A. S., Bauer, J. E., Sleighter, R. L., Dickhut, R. M. & Hatcher, P. G. Technical note: molecular characterization of aerosol-derived water soluble organic carbon using ultrahigh resolution electrospray ionization Fourier transform ion cyclotron resonance mass spectrometry. *Atmos. Chem. Phys.* **8,** 5099–5111 (2008).
21. Mazzoleni, L. R., Ehrmann, B. M., Shen, X. H., Marshall, A. G. & Collett, J. L. Water-soluble atmospheric organic matter in fog: exact masses and chemical formula identification by ultrahigh-resolution Fourier transform ion cyclotron resonance mass spectrometry. *Environ. Sci. Technol.* **44,** 3690–3697 (2010).
22. Fuzzi, S. *et al.* A simplified model of the water soluble organic component of atmospheric aerosols. *Geophys. Res. Lett.* **28,** 4079–4082 (2001).
23. Gilardoni, S. *et al.* Characterization of organic ambient aerosol during MIRAGE 2006 on three platforms. *Atmos. Chem. Phys.* **9,** 5417–5432 (2009).
24. Aiken, A. C. *et al.* O/C and OM/OC ratios of primary, secondary, and ambient organic aerosols with high-resolution time-of-flight aerosol mass spectrometry. *Environ. Sci. Technol.* **42,** 4478–4485 (2008).
25. Shilling, J. E. *et al.* Loading-dependent elemental composition of alpha-pinene SOA particles. *Atmos. Chem. Phys.* **9,** 771–782 (2009).
26. Presto, A. A. *et al.* Intermediate-volatility organic compounds: a potential source of ambient oxidized organic aerosol. *Environ. Sci. Technol.* **43,** 4744–4749 (2009).
27. Chhabra, P., Flagan, R. C. & Seinfeld, J. H. Elemental analysis of chamber organic aerosol using the aerodyne high resolution mass spectrometer. *Atmos. Chem. Phys.* **10,** 4111–4131 (2010).
28. Sun, Y. *et al.* Size-resolved aerosol chemistry on Whistler Mountain, Canada with a high-resolution aerosol mass spectrometer during INTEX-B. *Atmos. Chem. Phys.* **9,** 3095–3111 (2009).
29. Chen, Q. *et al.* Mass spectral characterization of submicron biogenic organic particles in the Amazon Basin. *Geophys. Res. Lett.* **36,** L20806 (2009).
30. Donahue, N. M., Epstein, S. A., Pandis, S. N. & Robinson, A. L. A two-dimensional volatility basis set: 1. organic-aerosol mixing thermodynamics. *Atmos. Chem. Phys. Discuss.* **10,** 24091–24133 (2010).
31. Goldstein, A. H. & Galbally, I. E. Known and unexplored organic constituents in the Earth's atmosphere. *Environ. Sci. Technol.* **41,** 1514–1521 (2007).
32. Atkinson, R. Rate constants for the atmospheric reactions of alkoxy radicals: an updated estimation method. *Atmos. Environ.* **41,** 8468–8485 (2007).
33. Lambe, A. T., Miracolo, M. A., Hennigan, C. J., Robinson, A. L. & Donahue, N. M. Effective rate constants and uptake coefficients for the reactions of organic molecular markers (n-alkanes, hopanes, and steranes) in motor oil and diesel primary organic aerosols with hydroxyl radicals. *Environ. Sci. Technol.* **43,** 8794–8800 (2009).
34. MacCarthy, P. The principles of humic substances. *Soil Sci.* **166,** 738–751 (2001).
35. Reemtsma, T., These, A., Springer, A. & Linscheid, M. Fulvic acids as transition state of organic matter: indications from high resolution mass spectrometry. *Environ. Sci. Technol.* **40,** 5839–5845 (2006).
36. Graber, E. R. & Rudich, Y. Atmospheric HULIS: how humic-like are they? A comprehensive and critical review. *Atmos. Chem. Phys.* **6,** 729–753 (2006).

37. Trainer, M. G. *et al.* Organic haze on Titan and the early Earth. *Proc. Natl Acad. Sci. USA* **103,** 18035–18042 (2006).
38. Kroll, J. H. *et al.* Measurement of fragmentation and functionalization pathways in the heterogeneous oxidation of oxidized organic aerosol. *Phys. Chem. Chem. Phys.* **11,** 8005–8014 (2009).
39. Kessler, S. H. *et al.* Chemical sinks of organic aerosol: kinetics and products of the heterogeneous oxidation of erythritol and levoglucosan. *Environ. Sci. Technol.* **44,** 7005–7010 (2010).
40. Pankow, J. & Asher, W. SIMPOL.1: a simple group contribution method for predicting vapor pressures and enthalpies of vaporization of multifunctional organic compounds. *Atmos. Chem. Phys.* **8,** 2773–2796 (2008).
41. Cappa, C. D. & Jimenez, J. L. Quantitative estimates of the volatility of ambient organic aerosol. *Atmos. Chem. Phys.* **10,** 5409–5424 (2010).
42. Aschmann, S. M., Atkinson, R. & Arey, J. Products of reaction of OH radicals with α-pinene. *J. Geophys Res. Atmos.* **107,** 4191 (2002).
43. Edney, E. O. *et al.* Polar organic oxygenates in PM2.5 at a southeastern site in the United States. *Atmos. Environ.* **37,** 3947–3965 (2003).
44. Surratt, J. D. *et al.* Chemical composition of secondary organic aerosol formed from the photooxidation of isoprene. *J. Phys. Chem. A* **110,** 9665–9690 (2006).
45. Kleindienst, T. E. *et al.* Estimates of the contributions of biogenic and anthropogenic hydrocarbons to secondary organic aerosol at a southeastern U.S. location. *Atmos. Environ.* **41,** 8288–8300 (2007).
46. Szmigielski, R. *et al.* 3-Methyl-1,2,3-butanetricarboxylic acid: an atmospheric tracer for terpene secondary organic aerosol. *Geophys. Res. Lett.* **34,** L24811 (2007).
47. Paulot, F. *et al.* Isoprene photooxidation: new insights into the production of acids and organic nitrates. *Atmos. Chem. Phys.* **9,** 1479–1501 (2009).
48. Claeys, M. *et al.* Terpenylic acid and related compounds from the oxidation of α-pinene: implications for new particle formation and growth above forests. *Environ. Sci. Technol.* **43,** 6976–6982 (2009).

Acknowledgements

This work was supported by the US Environmental Protection Agency (EPA) Science To Achieve Results (STAR) program (grant R833746 to J.H.K., N.M.D., D.R.W.), the US Department of Energy (DOE: grant DE-FG02-05ER63995), the National Science Foundation (NSF: grant ATM-0904292 to C.E.K., D.R.W. and M.R.C.; grants ATM-0449815 and ATM-0919189 to J.L.J.) and the National Oceanic and Atmospheric Administration (NOAA: grant NA08OAR4310565). K.R.W., H.B., E.R.M. and J.D.S are supported by the Director, Office of Energy Research, Office of Basic Energy Sciences, and Chemical Sciences Division of the US DOE (contract no. DE-AC02-05CH11231), with additional support from the Laboratory Directed Research and Development Program at the Lawrence Berkeley National Laboratory (LBNL). J.D.S. was also supported by the Camille and Henry Dreyfus foundation postdoctoral program in environmental chemistry. This paper has not been subject to peer and policy review by the above agencies, and therefore does not necessarily reflect their views; no official endorsement should be inferred.

Author contributions

The present work was originally conceived by J.H.K. with C.E.K. and D.R.W., with substantial input by N.M.D., J.L.J., M.R.C., S.H.K. and K.R.W. The ESI data were provided by K.E.A., L.R.M. and A.S.W. (Table 1 and Fig. 2). S.H.K. carried out the combinatorial calculations to produce Fig. 3. Data on the aging of organics (Fig. 4) were collected by J.D.S., S.H.K., J.H.K. and K.R.W. (squalane, triacontane and levoglucosan) and E.R.M., J.D.S., K.R.W. and H.B. (coronene). J.H.K. wrote the paper with input from all co-authors, especially N.M.D., J.L.J., M.R.C. and C.E.K. The Supplementary Information was written by J.H.K., N.M.D., H.B. and E.R.M.

Additional information

The authors declare no competing financial interests. Supplementary information accompanies this paper at www.nature.com/naturechemistry. Reprints and permission information is available online at http://npg.nature.com/reprintsandpermissions/. Correspondence and requests for materials should be addressed to J.H.K.

nature chemistry

SUPPLEMENTARY INFORMATION

DOI: 10.1038/NCHEM.948

Supplementary Information for

Carbon oxidation state as a metric for describing the chemistry of atmospheric organic aerosol

J. H. Kroll *et al*.

I) Relationship of $\overline{OS}_C$-n_C space to other proposed two-dimensional spaces for describing organic aerosol.

Several two-dimensional spaces have recently been proposed in an effort to consolidate the immense complexity of atmospheric organic species in ways that are conceptually or computationally tractable. These spaces are designed to assist calculations of important quantities such as concentrations of organic aerosol, to facilitate comparisons of measurements and model predictions, and/or to guide and enhance our fundamental understanding of the complex processes of organic degradation in the atmosphere. These approaches are complementary; each provides useful insight while sacrificing other details for the sake of simplicity. Here we summarize these spaces, and discuss the unique role of $\overline{OS}_C$ and the $\overline{OS}_C$-n_C space presented in this work.

The first such space proposed was the "carbon number-polarity grid" of Pankow and Barsanti[1]. The purpose of this space is to provide simple yet accurate predictions of organic thermodynamic properties (vapor pressure and activity coefficients in mixtures). If one wants to predict thermodynamic properties with the minimum number of independent pieces of information, carbon number and dipole moment are a natural combination. Chemical evolution is fundamentally external to this space; it is designed to complement chemical mechanisms that predict concentrations of either all relevant compounds via an explicit chemical mechanism[2], or a subset of surrogate compounds designed to represent the full set of organics[3].

DOI: 10.1038/NCHEM.948

A second two-dimensional space, based on volatility (C*) and the oxygen-to-carbon molar ratio (O/C), is described by Jimenez et al.[4]. This 2D volatility basis set (2DVBS) space is an extension of the volatility basis set developed by Donahue et al.[5]. In this framework, volatility is not predicted because it is the principal axis of the space; however, chemical reactions are considered based on whether they increase or decrease the volatility of reaction products relative to reactants. The second axis (O/C) allows for the degree of oxygenation of the organics to also be considered. The strength is that the consequences to phase partitioning are straightforward to see - the farther left in the space, the less volatile the material. This framework is fundamentally empirical, however. Chemical species are not directly identified (though they can be placed in the space), and trajectories associated with reaction mechanisms follow complex pathways through the space even for chemically straightforward sequences. The framework thus emphasizes the consequences of a chemical mechanism at the expense of illuminating the mechanism itself.

A third two-dimensional framework for describing OA is the Van Krevelen (H/C vs. O/C) plot. Heald et al.[6] recently showed that bulk OA occupies a narrow region in Van Krevelen space, with the H/C and O/C ratios being tightly coupled for a wide range of OA types. This is a primarily descriptive framework, affording insight into the average chemical makeup of OA, as well as which individual compounds may (or may not) be broadly representative of OA as a whole. Atmospheric aging appears to involve well-defined movement in Van Krevelen space (along a line with a slope of -1). However such movement is difficult to interpret in terms of the underlying chemical reactions, since carbon number of the organic molecules (which changes for many classes of reactions) is not represented in this space.

The above three frameworks are aimed at the description and/or modeling of key properties of organic aerosol. The $\overline{\mathrm{OS}}_C$-n_C space differs from these in that it is a fundamentally

chemical space, providing insight into the chemical changes that atmospheric organics undergo in the atmosphere. Such changes include reactions in which oxygenated functional groups are added to a carbon backbone (functionalization), association reactions between organic molecules to increase the number of carbon atoms in a molecule (oligomerization), and degradation processes in which the carbon number decreases (fragmentation). $\overline{\mathrm{OS}}_{\mathrm{C}}$-$n_C$ space is the only proposed two-dimensional OA framework for which these classes of reactions are uniquely defined by their trajectories: oligomerization moves material to the left, functionalization straight up, and fragmentation to the right. Such reactions cannot be generally defined in the other 2D spaces; for example, individual classes of reactions can involve either increases or decreases in polarity and volatility (such as the addition of new functional groups vs. oxidation of a functional group to a less polar one), so are not defined by an overall directionality in carbon number-polarity or 2DVBS spaces. Similarly, as described above, oligomerization and fragmentation reactions cannot be easily represented in Van Krevelen space. By contrast, these reaction types may be simply and unambiguously described in terms of their changes in $\overline{\mathrm{OS}}_{\mathrm{C}}$ and n_{C} (Figure 1 inset). Thus, by describing organics in terms of their fundamental chemical properties (the number and degree of oxidation of carbon atoms), $\overline{\mathrm{OS}}_{\mathrm{C}}$-$n_C$ space provides a powerful framework for interpreting proposed reaction pathways and OA composition data in terms of the key underlying chemical aging reactions.

DOI: 10.1038/NCHEM.948

II) Determination of Average Carbon Oxidation State of Atmospheric Organics (Table 1 and Figure 2)

a) ***HR-AMS***: For laboratory and ambient measurements of OA using the high-resolution aerosol mass spectrometer[7-12], $\overline{OS}_C$ was determined from Eq. 2 ($\overline{OS}_C$ = 2 O/C-H/C), with O/C and H/C of the OA determined using the approach of Aiken, et al.[7]. The range of values given is the highest and lowest reported for each aerosol type. The influence of heteroatoms (namely nitrogen) on $\overline{OS}_C$ is negligible, due to low measured abundances (N/C < 0.02)[7]. Errors in $\overline{OS}_C$ associated with heteroatom-containing groups are also likely to be minimal because atoms in weakly-bound species (such as organonitrates or organosulfates) tend not to be measured or tabulated as "organic" using thermal methods[13].

b) ***CHNS***: For the combustion analysis of HULIS samples[14,15], $\overline{OS}_C$ was determined from Eq. 2 ($\overline{OS}_C$ = 2 O/C-H/C). Inclusion of nitrogen introduces only a small uncertainty to the calculation of $\overline{OS}_C$, due to its low abundance (N/C≈0.04)[14,15]: assuming N is fully oxidized (OS_N = +5) leads to a 0.2 decrease in calculated $\overline{OS}_C$, whereas assuming N is fully reduced (OS_N = -3) leads to a 0.15 increase. Such errors are likely within the uncertainty of the $\overline{OS}_C$ determination. In the case of SOA from alkene oxidation[16], generated under high-NO_x conditions, the particulate nitrogen is almost certainly in the form or organic nitrates (OS_N=+5), so $\overline{OS}_C$ was determined by Eq. 1: $\overline{OS}_C$ = 2 O/C-H/C-5 N/C. Use of Eq. 2 (ignoring N and tabulating all nitrate oxygen as "organic") leads to a calculated $\overline{OS}_C$ that is higher by 0.5. We believe this represents an upper limit to the error introduced by neglecting organic nitrogen, due to the very high nitrogen abundance of the sample (N/C=0.1), and the fact that other techniques (AMS and possibly ESI as well) do not normally tabulate nitrate oxygen as "organic".

c) ***Ultrahigh resolution ESI-MS***: Values of $\overline{OS}_C$ from electrospray ionization mass spectrometry were determined from speciated molecular data described in refs. 17-22. Negative ion mode ESI data are used in all cases; for isoprene ozonolysis[21] and rainwater WSOC[18], data from positive ion mode ESI are also included. Details of sampling, extraction, and mass spectrometric analysis are provided in the individual publications. Average elemental ratios (O/C and H/C) of the samples were estimated using the approach described by Bateman, et al.[20], and were converted to $\overline{OS}_C$ using Eq. 2 ($\overline{OS}_C$ = 2 O/C-H/C). This averaging of elemental ratios is subject to errors arising from variations in ESI-MS response factors for different compounds; for the large number (hundreds to thousands) of compounds in these samples, such differences may approximately average out, though further characterization of ESI response factors is necessary to better constrain this. For ambient measurements, compounds with heteroatoms (N, S, and P) were excluded for simplicity, since the ranges in possible oxidation states of these atoms introduce some uncertainty to the $\overline{OS}_C$ of a given molecule. However the effects of these heteroatoms on calculated $\overline{OS}_C$ of the OA are generally small, due to their relatively low abundances, and the fact that most heteroatom-containing functional groups ($-ONO_2$, $-NH_2$, $-OSO_3H$, etc.) have only a minimal effect (+1 or -1) on the oxidation state of the adjacent carbon atom. Such effects will be investigated in detail in future work. In addition to the average values of $\overline{OS}_C$ given in Table 1, individual organic compounds in ambient aerosol[19] and fogwater[22] are shown in Figure 2.

DOI: 10.1038/NCHEM.948

III) Determination of Average Carbon Oxidation State and Carbon Number for the multigenerational oxidation of organics (Figure 4)

a) OH + isoprene and OH +α-pinene. Speciated oxidation products shown in Figure 4 include known carbonyl products of isoprene oxidation (methacrolein/methyl vinyl ketone, methylglyoxal, and glyoxal) as well as multifunctional species measured in laboratory studies of isoprene + OH[23,24] and α-pinene + OH[25-29]. Both gas-phase and particulate products are shown; for simplicity, only species with contiguous carbon skeletons (in which all carbon atoms are connected to each other) with $n_C \geq 2$ (isoprene) or $n_C \geq 5$ (α-pinene) are shown. Multifunctional products measured in other studies[30-34] have the same values of $\overline{OS}_C$ and n_C as the products shown.

b) OH + organic particles (squalane, triacontane, levoglucosan). Particles composed of single organics (squalane and triacontane, $C_{30}H_{62}$, and levoglucosan, $C_6H_{10}O_5$) were heterogeneously oxidized in a flow reactor, described in detail by Smith, *et al*.[35] (squalane) and Kessler, et al.[36] (levoglucosan). Oxidation of triacontane was carried out using the same approach as that of squalane[35] except that triacontane particles were generated upstream of the reactor using a nucleation oven at 140°C, with the aerosol stream passed through a second annealing oven (T=75°C) in order to make the particles more spherical in shape.

Average $\overline{OS}_C$ of the particulate organics was determined using Equation 2 and AMS measurements of O/C and H/C ratios. The average number of carbons per molecule (n_C) was determined by assuming fractional changes in carbon number are equal to the fraction of carbon remaining in the particle phase after oxidation. This assumption is broadly consistent with measured changes to particle volatility upon heterogeneous oxidation, which indicate that carbon

loss from heterogeneous oxidation occurs via the release of small volatile fragments from the particulate organics[37].

c) OH, O_3 + coronene films. The XPS investigations of the oxidation of coronene by ozone and OH are discussed in detail by Mysak, *et al.*[38]. The XPS measurements were performed using the Ambient Pressure Photoemission Spectrometer at beamline 11.0.2 at the Advanced Light Source in Berkeley, CA[39]. Thin films of coronene (97% purity, Sigma Aldrich) were vapor-deposited on clean polycrystalline Au foil or Ag(111) single crystal substrates at a deposition rate of ~0.2 Å min^{-1}, as measured by a quartz crystal microbalance. This growth rate yielded consistently homogenous films, as evidenced by both XPS and AFM measurements. The thickness of the unreacted coronene film was determined from the attenuation of the substrate signal using the inelastic mean free path (IMFP) of electrons in coronene at the given electron kinetic energy of 140 eV [40]. Using a IMFP value of 8.5 Å the thickness of the unreacted coronene film was found to be 4-6 Å [38].

Ozone is produced by passing O_2 through a commercial corona discharge source (Yanco). The ozone flow is then diluted with N_2 and introduced via a precision leak valve into the sample chamber at a concentration of ~1x10^8 molecules cm^{-3}. The ozone is directed at the surface through a Teflon doser located ~2 cm from the sample surface. OH is produced by passing N_2 through a water bubbler, selecting a portion of this flow with a leak valve, and passing it through a microwave discharge cavity and into the chamber via a 1.27 cm O.D. quartz tube ending 3 cm from the sample surface. The OH concentration is estimated to be 9.8 x 10^8 molecules cm^{-3}. The total operating pressure in the sample chamber for both the OH and O_3 experiments is fixed at 10^{-5} Torr. To measure heterogeneous kinetics, XPS spectra are collected as a function of reaction time at a fixed concentration of O_3 or OH. It was found that the OH reactions are sufficiently fast that it is necessary to turn off the OH source during the data collection period.

DOI: 10.1038/NCHEM.948

In contrast, the O_3 reaction proceeded slowly enough that the reaction is allowed to proceed continuously during data collection. Care was taken to avoid radiation-induced changes to the coronene films. The data shown in Fig. 4 were free of detectable radiation damage.

The values for n_C and $\overline{OS}_C$ were determined from C1s XPS data; examples of these spectra are shown in Fig. S1. The binding energy scale was calibrated by the Fermi energy of the Ag substrate. Fig. S1 shows C1s XPS spectra for the OH + coronene reaction at two reaction times, (a) 15 s and (b) 105 s. The C1s spectra are fit using five components, which were assigned to different carbon species (C=C, CH_x, C-OH, C=O and C(O)OH) according to their binding energy by comparing to literature values [41]. The validity of the assignment to those species was cross-checked by comparison to O 1s spectra (not shown), which also revealed the C-OH, C=O and C(O)OH species. $\overline{OS}_C$ was determined from measurements of elemental ratios (Eq. 2). The O/C ratio was determined directly from the C1s spectra by dividing the area of the O-related C1s peaks (with C(O)OH weighted by a factor of 2) by the peak area of the five C peaks; hydrogen atoms are not measured directly by XPS, so H/C was estimated by assuming each CH_x, C-OH, and C(O)OH carbon has one H atom, and C=C carbon has on average 0.5 H atoms (the same as coronene). The number of carbons (n_C) was determined from the ratio of the total C1s peak area of the reacted film to the peak area of the unreacted film, normalized to 24 (the number of C atoms in coronene). This method may slightly underestimate the value for n_C since it does not take into account possible attenuation of the C1s signal due to the presence of O in the reacted films. Since it is not possible in these experiments to determine the relative positions of O and C atoms with respect to the surface, this effect cannot be quantified. However, we can estimate the upper limit for the error in the n_C measurements from the maximum value for the O/C ratio (~0.7) by assuming that all C are located at the substrate interface in one layer, while all O are

located on top of the carbons, also in one layer. We estimate that for that extreme case the value for n_C is underestimated by less than 15%.

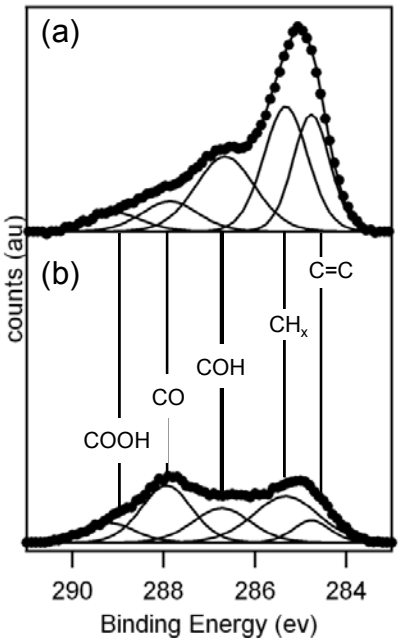

Fig. S1: C1s XPS spectra for the OH + coronene reaction at two reaction times, (a) 15 s and (b) 105 s. The C1s spectrum is fit using five components (C=C, CH_x, C-OH, C=O and C(O)OH). The data were taken with an incident photon energy of 430 eV.

References Cited

1. Pankow, J.F. & Barsanti, K.C. The Carbon Number-Polarity Grid: A Means to Manage the Complexity of the Mix of Organic Compounds When Modeling Atmospheric Organic Particulate Matter. *Atmos. Environ.* **43**, 2829-2835 (2009).
2. Aumont, B., Szopa, S. & Madronich, S. Modelling the evolution of organic carbon during its gas-phase tropospheric oxidation: development of an explicit model based on a self generating approach. *Atmospheric Chemistry and Physics* **5**, 2497-2517 (2005).
3. Griffin, R., Dabdub, D. & Seinfeld, J. Secondary organic aerosol - 1. Atmospheric chemical mechanism for production of molecular constituents. *Journal of Geophysical Research-Atmospheres* **107**, (2002).
4. Jimenez, J.L. et al. Evolution of Organic Aerosols in the Atmosphere. *Science* **326**, 1525-1529 (2009).
5. Donahue, N., Robinson, A., Stanier, C. & Pandis, S. Coupled partitioning, dilution, and chemical aging of semivolatile organics. *Environmental Science and Technology* **40**, 2635-2643 (2006).
6. Heald, C.L. et al. A simplified description of the evolution of organic aerosol composition in the atmosphere. *Geophys. Res. Lett.* **37**, L08803, doi:10.1029/2010GL04273 (2010).
7. Aiken, A.C. et al. O/C and OM/OC ratios of primary, secondary, and ambient organic aerosols with high-resolution time-of-flight aerosol mass spectrometry. *Environ. Sci.*

Technol. **42**, 4478-4485 (2008).
8. Chhabra, P., Flagan, R.C. & Seinfeld, J.H. Elemental analysis of chamber organic aerosol using the Aerodyne High Resolution Mass Spectrometer. *Atmos. Chem. Phys.* **10**, (2010).
9. Chen, Q. et al. Mass spectral characterization of submicron biogenic organic particles in the Amazon Basin. *Geophys. Res. Lett.* **36**, (2009).
10. Presto, A.A. et al. Intermediate-Volatility Organic Compounds: A Potential Source of Ambient Oxidized Organic Aerosol. *Environ. Sci. Technol.* **43**, 4744-4749 (2009).
11. Shilling, J.E. et al. Loading-dependent elemental composition of alpha-pinene SOA particles. *Atmos. Chem. Phys.* **9**, 771-782 (2009).
12. Sun, Y. et al. Size-resolved aerosol chemistry on Whistler Mountain, Canada with a high-resolution aerosol mass spectrometer during INTEX-B. *Atmos. Chem. Phys.* **9**, 3095-3111 (2009).
13. Farmer, D.K. et al. Response of the aerosol mass spectrometer to organonitrates and organosulfates and implications for field studies. *Proc. Natl. Acad. Sci. USA* **107**, 6670-6675 (2010).
14. Kiss, G., Varga, B., Galambos, I. & Ganszky, I. Characterization of water-soluble organic matter isolated from atmospheric fine aerosol. *J. Geophys Res. Atmos.* **107**, (2002).
15. Krivacsy, Z. et al. Study on the chemical character of water soluble organic compounds in fine atmospheric aerosol at the Jungfraujoch. *J. Atmos. Chem.* **39**, 235-259 (2001).
16. O'Brien, R.J., Holmes, J.R. & Bockian, A.H. Formation of Photochemical Aerosol from Hydrocarbons - Chemical Reactivity and Products. *Environ. Sci. Technol.* **9**, 568-576 (1975).
17. Altieri, K. et al. Oligomers formed through in-cloud methylglyoxal reactions: Chemical composition, properties, and mechanisms investigated by ultra-high resolution FT-ICR mass spectrometry. *Atmospheric Environment* **42**, 1476-1490 (2008).
18. Altieri, K.E., Turpin, B.J. & Seitzinger, S.P. Oligomers, organosulfates, and nitrooxy organosulfates in rainwater identified by ultra-high resolution electrospray ionization FT-ICR mass spectrometry. *Atmos. Chem. Phys.* **9**, 2533-2542 (2009).
19. Wozniak, A.S., Bauer, J.E., Sleighter, R.L., Dickhut, R.M. & Hatcher, P.G. Technical Note: Molecular characterization of aerosol-derived water soluble organic carbon using ultrahigh resolution electrospray ionization Fourier transform ion cyclotron resonance mass spectrometry. *Atmos. Chem. Phys.* **8**, 5099-5111 (2008).
20. Bateman, A.P., Nizkorodov, S.A., Laskin, J. & Laskin, A. Time-Resolved Molecular Characterization of Limonene/Ozone Aerosol using High-Resolution Electrospray Ionization Mass Spectrometry. *Phys. Chem. Chem. Phys.* **11**, (2009).
21. Nguyen, T.B. et al. High-resolution mass spectrometry analysis of secondary organic aerosol generated by ozonolysis of isoprene. *Atmos. Environ.* **44**, 1032-1042 (2010).
22. Mazzoleni, L.R., Ehrmann, B.M., Shen, X.H., Marshall, A.G. & Collett, J.L. Water-Soluble Atmospheric Organic Matter in Fog: Exact Masses and Chemical Formula Identification by Ultrahigh-Resolution Fourier Transform Ion Cyclotron Resonance Mass Spectrometry. *Environ. Sci. Technol.* **44**, 3690-3697 (2010).
23. Surratt, J.D. et al. Chemical composition of secondary organic aerosol formed from the photooxidation of isoprene. *J. Phys. Chem. A* **110**, 9665-9690 (2006).
24. Paulot, F. et al. Isoprene photooxidation: new insights into the production of acids and organic nitrates. *Atmos. Chem. Phys.* **9**, 1479-1501 (2009).
25. Aschmann, S.M., Atkinson, R. & Arey, J. Products of reaction of OH radicals with a-pinene. *J. Geophys Res. Atmos.* **107**, (2002).
26. Edney, E.O. et al. Polar organic oxygenates in PM2.5 at a southeastern site in the United States. *Atmos. Environ.* **37**, 3947-3965 (2003).
27. Kleindienst, T.E. et al. Estimates of the Contributions of Biogenic and Anthropogenic

Hydrocarbons to Secondary Organic Aerosol at a Southeastern U.S. Location. *Atmos. Environ.* **41**, 8288-8300 (2007).
28. Szmigielski, R. et al. 3-methyl-1,2,3-butanetricarboxylic acid: An atmospheric tracer for terpene secondary organic aerosol. *Geophys. Res. Lett.* **34**, L24811, doi:10.1029/2007GL031338 (2007).
29. Claeys, M. et al. Terpenylic Acid and Related Compounds from the Oxidation of alpha-Pinene: Implications for New Particle Formation and Growth above Forests. *Environ. Sci. Technol.* **43**, 6976-6982 (2009).
30. Tuazon, E. & Atkinson, R. A Product Study of the Gas-Phase Reaction of Isoprene with the OH Radical in the Presence of NOx. *International Journal of Chemical Kinetics* **22**, 1221-1236 (1990).
31. Ruppert, L. & Becker, K. A product study of the OH radical-initiated oxidation of isoprene: formation of C-5-unsaturated diols. *Atmospheric Environment* **34**, 1529-1542 (2000).
32. Zhao, J., Zhang, R., Fortner, E. & North, S. Quantification of hydroxycarbonyls from OH-isoprene reactions. *Journal of the American Chemical Society* **126**, 2686-2687 (2004).
33. Surratt, J. et al. Organosulfate formation in biogenic secondary organic aerosol. *Journal of Physical Chemistry A* **112**, 8345-8378 (2008).
34. Paulot, F. et al. Unexpected Epoxide Formation in the Gas-Phase Photooxidation of Isoprene. *Science* **325**, 730-733 (2009).
35. Smith, J. et al. The heterogeneous reaction of hydroxyl radicals with sub-micron squalane particles: a model system for understanding the oxidative aging of ambient aerosols. *Atmospheric Chemistry and Physics* **9**, 3209-3222 (2009).
36. Kessler, S.H. et al. Chemical Sinks of Organic Aerosol: Kinetics and Products of the Heterogeneous Oxidation of Erythritol and Levoglucosan. *Environ. Sci. Technol.* **44**, 7005-7010 (2010).
37. Kroll, J.H. et al. Measurement of fragmentation and functionalization pathways in the heterogeneous oxidation of oxidized organic aerosol. *Phys. Chem. Chem. Phys.* **11**, 8005-8014 (2009).
38. Mysak, E.R. et al. Competitive Reaction Pathways for Functionalization and Volatilization in the Heterogeneous Oxidation of Coronene Thin Films by Hydroxyl Radicals and Ozone. *Manuscript in preparation* (2010).
39. Ogletree, D., Bluhm, H., Hebenstreit, E. & Salmeron, M. Photoelectron spectroscopy under ambient pressure and temperature conditions. *Nucl. Instrum. Methods Phys. Res., Sect. A* **601**, 151-160 (2009).
40. Powell, C. & Jablonsk, I. *NIST Electron Inelastic-Mean-Free-Path Database - Version 1.1*. (National Institute of Standards and Technology: Gaithersburg, MD, 2000).
41. Briggs, D. & Beamson, G. *High Resolution XPS of Organic Polymers: The Scienta ESCA300 Database*. (John Wiley & Sons: New York, 1992).